Microphysical processes involving the vapour phase dominate in simulated low-level Arctic clouds

Theresa Kiszler[1], Davide Ori[1], and Vera Schemann[1]

[1]University of Cologne, Institute of Geophysics and Meteorology, 50939 Cologne, Germany

Correspondence: Theresa Kiszler (tkiszler@uni-koeln.de) and Vera Schemann (vera.schemann@uni-koeln.de)

Abstract. Current general circulation models struggle to capture the phase-partitioning of clouds accurately, ~~either overestimating or~~ both overestimating and underestimating the supercooled liquid substantially. This impacts the radiative properties of clouds. Therefore, it is of interest to understand which processes determine the phase-partitioning. In this study, microphysical process rates are analyzed to study what role each phase-changing process plays in low-level Arctic clouds. Several months of cloud-resolving ICON simulations using a two-moment cloud microphysics scheme, are evaluated. The microphysical process rates are extracted using a diagnostic tool introduced here, which runs only the microphysical parameterisation using previously simulated days. It was found that the ~~importance of a process varies for the polar night and polar day, although phase changes that involve~~ processes impacting ice are more efficient during polar night than polar day. For the mixed-phase clouds (MPCs) it became clear that phase changes involving the vapour phase ~~dominate~~dominated in contrast to processes between liquid and ice. Computing the rate of the Wegener-Bergeron-Findeisen process further indicated that the MPCs frequently (42 %) seemed to be glaciating. Additionally, the dependence of each process on the temperature, vertical wind and saturation was evaluated. ~~Going a step further, we used the combined evaporation and deposition rates to demonstrate the Wegener-Bergeron-Findeisen process occurrence~~ This showed that especially the temperature influences the occurrence and interactions of different processes. This study helps to better understand how microphysical processes act in different regimes. It additionally shows which processes play an important role ~~and contribute~~ in contributing to the phase-partitioning in ~~low-level Arctic~~ Arctic low-level mixed-phase clouds. Therefore, these processes ~~can~~ could potentially be better targeted for improvements in the ICON model that aim to ~~better~~ more accurately represent the phase-partitioning of Arctic low-level mixed-phase clouds.

1 Introduction

Several studies (Ebell et al., 2020; Shupe and Intrieri, 2004; Curry and Ebert, 1992) showed the importance of clouds for the Arctic radiative budget. Clouds further play a role in different feedback mechanisms, for instance, the cloud-phase feedback (Mitchell et al., 1989), and either amplify (positive feedback) or dampen (negative feedback) the warming. As the Arctic is warming up to four times faster than the global average (Rantanen et al., 2022), it is of interest to which extent clouds play a role. Currently, the question still remains though whether the total cloud feedback is positive or negative (Middlemas et al., 2020; Goosse et al., 2018). A specific challenge is the cloud-phase feedback as the changes in the cloud's phase-partitioning impact the cloud radiative effect (Mitchell et al., 1989; Storelvmo et al., 2015). The reason for these uncertainties regarding

the cloud feedbacks stems from the difficulties of models on all scales to represent clouds, especially mixed-phase clouds (MPCs) accurately (Kay et al., 2016; Zelinka et al., 2020). These difficulties are connected to the complexity of microphysical processes in clouds and their parameterisations in models. One consequence is that many models are unable to capture the phase-partitioning in clouds correctly (Tan et al., 2016). As a result, it is hard to quantify cloud feedbacks causing uncertainties in the climate projections (Zelinka et al., 2020).

Some models struggle to represent supercooled liquid in MPCs and often underestimate it (Cesana and Chepfer, 2012; Kiszler et al., 2023). Huang et al. (2021) link this underestimation of cloud liquid in the CESM1 model to the Wegener-Bergeron-Findeisen (WBF) process, where ice grows at the expense of liquid water due to the lower saturation required above frozen surfaces. While sometimes the limited spatial and temporal resolution can cause the full glaciation of a cloud (Storelvmo and Tan, 2015), other studies showed the importance of the ice nucleation and WBF process to estimate the climate forcing of ~~MPC~~ MPCs correctly (Shaw et al., 2022; McGraw et al., 2023). In contrast, Zhang et al. (2020) found an overestimation of liquid in the E3SM model after several changes, including a switch in the ice nucleation scheme ~~(new: Classical Nucleation Theory, Wang et al., 201~~ and microphysical parameterisation scheme~~(new: Gettelman and Morrison, 2015)~~. Again, this shows that the phase-partitioning and representation of cloud microphysical processes remains a challenge (Korolev et al., 2017; Morrison et al., 2020).

To understand where these uncertainties come from and address them, many studies have used sensitivity tests by varying process parameters or aerosol concentrations, where the subsequent changes of the cloud macro- and microphysics and other model components are evaluated (e.g. Lasher-Trapp et al., 2018; Shaw et al., 2022). This can provide valuable insights but makes it hard to untangle the exact contribution of each process. Additionally, the number of feasible model runs cannot cover the full range of possible parameter changes and combinations. Another approach aims to evaluate the microphysical process rates directly. This was done, for instance, by Gettelman et al. (2013) for a general circulation model (GCM) to look at the relative importance of microphysical processes in climate models using daily rates. In a recent paper, Barrett and Hoose (2023) used so-called microphysical pathways, which include different sets of microphysical processes, to study an idealized deep convective system. Kalesse et al. (2016) found a strong connection between the deposition rate of snow and the snow mass mixing ratio in a case study of an Arctic low-level cloud. Fan et al. (2017) studied the effect of changing ice nucleating particles (INP) and cloud condensation nuclei (CCN) concentrations on process rates, finding an increase in condensation, evaporation, deposition, sublimation and riming with increasing aerosols.

This study uses microphysical process rates to determine which processes contribute most to phase changes in Arctic low-level clouds (LLC). The focus lies on Svalbard, where LLCs frequently occur (Gierens et al., 2020; Nomokonova et al., 2019). Svalbard has an above average occurrence of MPCs (45-60 %) in comparison to the rest of the Arctic (30-50 %, Mioche et al., 2015) making the location ideal for studying the phase-partitioning of clouds. Cloud-resolving simulations with ICON-LEM (ICOsahedral Nonhydrostatic model in the large-eddy version, Dipankar et al. (2015)) are used to explore the importance of the microphysical processes for the phase-partitioning. To achieve this, a diagnostic tool is introduced, which provides the process rates using the simulation output as input. Several aspects are taken into account in the evaluation, those are the

difference between polar night and day, temperature, vertical wind and saturation regimes. Additionally, we use the deposition and evaporation rates to evaluate if and how the WBF process impacts the amount of liquid and frozen hydrometeors in the simulated clouds.

2 Methods and data

2.1 ~~Model~~ ICON simulations~~and data selection~~

The ICON-LEM (Dipankar et al., 2015; Heinze et al., 2017) simulations which we performed cover a circular domain with ~~approx.~~ approximately 100 km diameter centred in Ny-Ålesund (Svalbard, lon-lat) and run with ~~approx.~~ approximately 600 m resolution. The general setup follows the papers by Kiszler et al. (2023) and Schemann and Ebell (2020) ~~with each simulation covering~~ and a thorough evaluation of the model performance is provided in those studies. While the general performance of the model was found to be very good, there were some short comings. In Kiszler et al. (2023) it is shown that the cloud occurrence matches the observations well but that the occurrence of liquid containing clouds is underestimated by around 30 %. Each simulation covers 24 h, although the first 3 hours are excluded in the analysis to avoid the spin-up. The ~~forcing is from a~~ initial and boundary conditions for each ICON-LEM limited area simulation are provided by an ICON-NWP simulation with 2.4 km resolution. This ICON-NWP simulation ~~, which is run on~~ covers a larger domain and is forced by the operational German weather service global ICON-NWP runs. The turbulence is parameterised by a 3D-Smagorinsky scheme (Dipankar et al., 2015). The two-moment scheme from Seifert and Beheng (2006) with an added hail class Blahak (2008) is used for the microphysics (referred to as SB). ~~A slight adaptation was made to the default ICON microphysical settings.~~ We use the Segal and Khain (2006) cloud condensation nuclei (CCN) activation with maritime aerosols, as well as the heterogeneous ice nucleation from Phillips et al. (2008) with the maritime aerosol concentrations. The output is given in the form of the vertical column above the grid cell containing Ny-Ålesund (meteogram) for every 9 s on 150 levels. This output includes the following hydrometeor mass mixing ratios and number concentrations: cloud droplets, rain, ice, snow, graupel and hail.

2.2 Selected data

For the analysis, a subset of the data, which only includes low-level clouds, was created. This was done by first selecting all grid boxes which are cloudy using a threshold for the hydrometeor concentration of 10^{-8} kg kg^{-1} (same as in Kiszler et al., 2023; Schemann and Ebell, 2020) above which a grid box is defined as cloudy. For a cloud to be classified as low-level, the cloud top height must be below 2.5 km (same as Gierens et al., 2020; Chellini et al., 2022). Additionally, precipitating hydrometeors are not differentiated from non-precipitating ones. Therefore, a cloud with rain, graupel, hail or snow that reaches the ground will have a cloud base height at the ground. Further, if there is a cloud with a cloud top height higher than 2.5 km above the low cloud, we only use these cases if the higher cloud's bottom height is at least 500 m higher than the low cloud's top height.

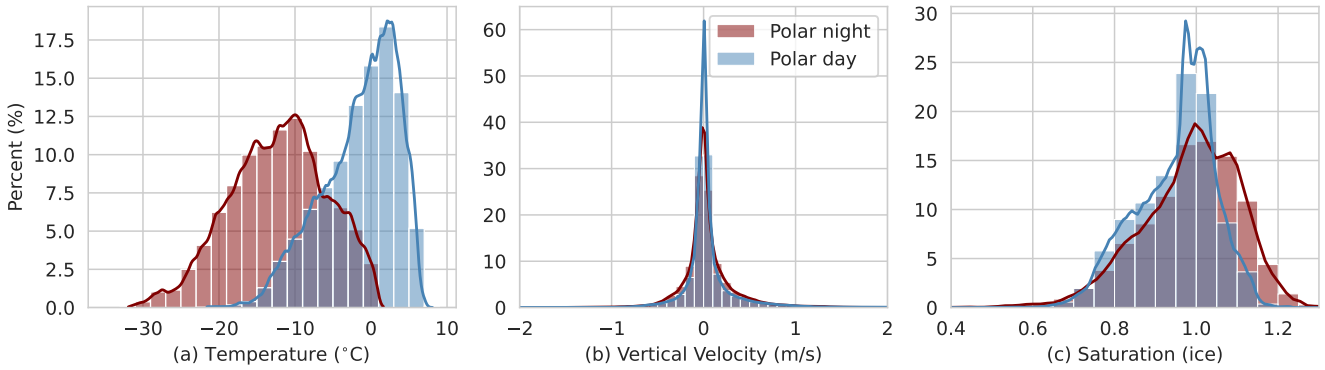

Figure 1. Distribution of the temperature (a), vertical velocity (b) and ice saturation ratio (c) for the polar night (PN, red) and polar day (PD, blue).

The frozen and liquid hydrometeors are grouped in the analysis to focus on phase transitions. The frozen mass mixing ratios ("frozen mass", kg kg^{-1}) is the sum of cloud ice, graupel, hail, and snow, and the liquid mass mixing ratios ("liquid mass", kg kg^{-1}) is the sum of cloud droplets and rain. Generally, the liquid and frozen mass mixing ratios lie between 10^{-8} and 10^{-3} kg kg−1. The occurrence of low-level clouds and their composition varies between seasons (Mioche et al., 2015). Therefore, two sets of data are used. One covers the polar night (PN, November 2021 - February 2022) and one the polar day (PD, May-August 2021). In total, for the ~~polar night~~PN, there are around 26.3 days' worth of low-level clouds, and for the ~~polar day~~PD, there are around 37.9 days. For the selection of the MPCs only cloudy pixels where both the liquid and frozen mass are above 10^{-8} kg kg^{-1} are chosen. Of the total 23.8 days' worth of MPCs, 14.1 occur during PN and 9.7 during PD.

In the analysis the temperature, vertical velocity, and ice/water saturation with dependency of different microphysical processes is discussed. These variables were chosen as the microphysical processes are directly connected to them. As PN and PD differ in parts strongly, a short overview of the thermodynamic conditions for the selected cloudy grid points is provided here. Fig. 1 a-c show the distributions of the temperature, vertical velocity, and ice saturation for the PN and PD. The PN temperature ranges from -32 to 2 °C with the mean at -14 °C. In contrast, the much warmer PD varies less (-22 to 8 °C) and has a mean value of -2 °C. The vertical velocity is narrowly arranged around 0 m s^{-1} for both PN and PD, and both the PD and PN low variation (standard deviation: PD 0.35 m s^{-1}, PN 0.29 m s^{-1}). Extremes, which happen very rarely, are found more in the upwards motion, with the overall maximum at 6.43 m s^{-1}. The saturation with respect to ice does not reach as high values during the PD as during the PN.

Of the total 26.3 days of low-level clouds during PN, almost all contain periods with frozen hydrometeors (25.4 days), and slightly more than half contain liquid hydrometeors (15.5 days, 58 %). For the 37.9 days of low-level clouds during PD, almost all times contained liquid (96 %) while only 31 % contained ice. This is connected to the fact that liquid occurs

at higher temperatures, which are more prevalent during the polar day (Fig. 1 a). Another aspect to note is that similar to Shupe et al. (2008) and as theorized by Korolev (2008), we found that higher upward vertical velocities are connected to higher saturation and with that also to higher hydrometeor masses (not shown). This already hints towards potential correlations between certain processes and the vertical wind and saturation which are presented in the results.

2.3 Microphysics parameterisation wrapper

To extract the process rates, this study uses a "microphysical parameterisation wrapper". The goal is to provide a simple diagnostic tool with spatial and temporal flexibility. Therefore, we chose to run the two-moment SB scheme and the saturation adjustment (for condensation/evaporation) independently from the model. A meteogram (single column) or 3D output file from a previous simulation can be used as input for the wrapper. The model output is provided as input to the microphysical scheme in each timestep and on the same vertical grid as used in the model. It computes a single timestep, writes out the rates and continues with the following timestep. This approach allows the use of previous simulations from which the meteogram or 3D output of the required variables exists. A flowchart is shown in Fig. A1.

This approach has the clear advantage of being very fast compared to rerunning a full simulation, and one can focus on single processes. Further, outputting an entire domain of microphysical process rates is extremely space-consuming in most cases and can be avoided by just using a spatial and/or temporal selection. ~~Another advantage is that the values of the thermodynamic variables (temperature T, pressure p, vertical velocity w, density ρ) are known exactly when they are used to compute the processes. This is not the case if one runs the entire model and outputs the thermodynamic variables only after additional physics and dynamical schemes have run.~~ Additionally, it is possible to explore potential sensitivities of microphysical processes by applying changes inside of the wrapper and using it as a test suite. As this tool is simplified and only captures a part of the model, the advantages come with some limitations. One must keep in mind that any transportation (advection and precipitation) of hydrometeors cannot be included as the model itself is not run. In this study, we are only interested in the microphysical processes. Therefore, this is not an issue.

The mass change due to a process is computed by taking the difference between the mass before and after the process and is called (ΔQ_{proc}). Here, a timestep (Δt) of 3 seconds is used for the time integration. Therefore, the process rate ($\frac{\Delta Q_{proc}}{\Delta t}$) is given as the hydrometeor mass mixing ratio change over 3 seconds and is denoted as the "tendency" (kg kg^{-1} 3s^{-1}) in the following sections. A minimum threshold for the tendency of $\frac{\Delta Q_{proc}}{\Delta t} > 10^{-18}$ kg kg^{-1} 3s^{-1} is set to avoid including numerical noise. This threshold is much lower than the threshold for the hydrometeor mass (10^{-8} kg kg^{-1}) as the microphysical process tendencies changing the mass can be very small. As mentioned before, the hydrometeors are summed up into a liquid and frozen mass. The same is done with the processes, meaning, for example, that deposition is the sum of deposition onto ice particles, snow, graupel and hail. In this study, only processes that cause phase changes are included, as we are interested in processes that contribute to the phase-partitioning. E.g. frozen collisions are not evaluated as all frozen hydrometeors are

summed up to a single class and compensate each other. Many of the processes evaluated in this study have self-explanatory names. Nevertheless, a brief process summary is given here and in Table 1 to prevent misunderstandings.

Deposition and Sublimation includes either the decrease or increase of water vapour due to phase changes from frozen to vapour. They are computed by the same process and split into negative (sublimation) and positive (deposition) contributions to the frozen mass.

Homogeneous and heterogeneous ice nucleation describes as one part the homogeneous nucleation of liquid aerosols, although it is rarely cold enough (T<30 °C) in the clouds used in this study to happen. The heterogeneous nucleation describes nucleation via immersion freezing and deposition nucleation. The parameterisation follows as mentioned Phillips et al. (2008). As homogeneous cloud droplet freezing did not occur for the low-level clouds, it is neglected here.

CCN activation describes the activation of cloud condensation nuclei following the parameterisation of Segal and Khain (2006).

Frozen evaporation and Melting refer to the melting of frozen hydrometeors, which can entail evaporation, but both are treated separately, leading to a process called "evaporation" also for the frozen hydrometeors.

Riming describes the accumulation of liquid mass on a frozen hydrometeor by decreasing the liquid mass and increasing the frozen mass. In SB in ICON, this also includes the Hallet-Mossop secondary ice production~~, and if~~ . If T>0 °C enhanced melting after riming will take place, making the frozen mass increase due to riming ~~smaller~~less as not all liquid will freeze onto the frozen hydrometeors.

Condensation and Evaporation includes either the decrease or increase of water vapour due to phase changes from cloud droplets and raindrops to vapour. They are the positive (condensation) and negative (evaporation) contributions of the saturation adjustment to the liquid mass.

Rain freezing only includes the freezing of raindrops and not cloud droplets. As both are summed up, though, this causes a decrease of the total liquid mass while the total frozen mass increases.

3 Results

3.1 Dominating processes in low-level clouds

We used a simple but straightforward approach to understand which processes dominate the phase-partitioning in low-level clouds. For each process, the mean value over all cases was computed. The mean values can vary, for instance, with temperature, as shown in the next section, so the percentage of occurrence ~~, where a process makes up for over 1 % of the total mass change,~~ is used as a second metric. The outcome of this is shown for all processes in Fig. 2 split into polar night (a and c) and polar day (b and d), as well as into MPCs (a and b) and pure frozen or liquid clouds (c and d). The further a process is towards the upper right corner, the more relevant it is considered to be. ~~One can see that there are some differences between the same processes for liquid and frozen hydrometeors. That is partially because some processes affect liquid, frozen and vapour at the same time, so the mean does not overlap in all cases. Additionally, there is numerical noise, which is why a minimum threshold for the tendency of $\frac{\Delta Q_{proc}}{\Delta t} > 10^{-18}$ kg kg^{-1} 3s^{-1} is set.~~ As mentioned earlier, only processes which contribute to

Process	ΔQ_L	ΔQ_F	ΔQ_v
Ice nucleation	-	+	-
CCN activation	+	/	-
Deposition	/	+	-
Sublimation	/	-	+
Evaporation	-	/	+
Condensation	+	/	-
Riming	-	+	/
Rain freezing	-	+	/
Melting	+	-	/

Table 1. Impact of each process on the hydrometeor masses for liquid (ΔQ_L) and frozen (ΔQ_F) as well as the water vapour (ΔQ_v). The liquid class contains cloud droplets and raindrops, the frozen class contains ice particles, snow, graupel, and hail. A plus indicates an increase in the hydrometeor mass, and a minus a decrease.

phase changes are included here. Further, we used the minimum of deposition and evaporation to compute the WBF tendency for the MPC cases.

What becomes very clear from Fig. 2 ~~a) and b) is that sublimation, deposition, and evaporation happen very frequently and also have the highest mean values. During the polar day (~~is that there is a hierarchy in how relevant a process is. In all cases evaporation seems to be strongest followed by deposition. Here, a striking difference between MPCs and single phase clouds becomes visible. While in liquid clouds it seems like the majority of the clouds are in the decaying phase, shown by the frequent evaporation (above 79 %) in contrast to condensation (below 21 %), this is not necessarily true for the MPCs. As Fig. 2 ~~b) it is visible that while evaporation and deposition still play a large role, sublimation has become less frequent. However, there is much less ice in general during the polar day, and most simulated cloudswere purely liquid during that time. Melting, evaporation due to melting, and rain freezing all show mean tendencies above 10^{-12} kg kg^{-1} but occur below 20 % of the time, although ~~a) and b) show, deposition is stronger in MPCs in contrast to the pure ice clouds, indicating that the MPCs are generally transitioning from liquid to ice. The transition from liquid to ice via the vapour phase can be quantified using the WBF tendency which shows a frequency of around 42 % and varies little between PN and PD. At the same time, the pure ice clouds seem to be in a more stable state although the higher frequency of sublimation indicates a slight decay also for the ice clouds. The finding that all cloud types seem to be in the process of decay, where processes acting as sinks are dominating, is potentially a local feature as only the single column of Ny-Ålesund is used here. This feature indicates that the microphysical processes may also have a strong location dependency. For instance, in Ny-Ålesund, the ~~differences between the seasons are striking. During the polar day, rain freezing and melting increase in importance, possibly due to the difference in temperature regimes, which allows more precipitation to melt or more liquid precipitation to occur, which can then freeze~~air over the fjord

is more moist than over the land (Kiszler et al., 2023), which may cause more evaporation over land if a cloud is advected there.

Another aspect, is that the microphysical process show different behaviours during the PN and PD. Processes involving the ice phase show a decreased mean tendency during PD in contrast to PN. Additionally, one can see that riming seems to be more frequent during the PN (30 %) than PD (21 %), while rain freezing is less frequent during the PN (PN: 32.0 % and PD: 38.64 %). Such differences between PN and PD are likely connected to the dependency of the processes on the temperature regime as discussed later. Ice and liquid ~~sources via nucleation~~formation via nucleation/activation tend to occur quite seldom, as one can see from the CCN activation (CCN act., in Fig. 2) and the homogeneous & heterogeneous nucleation (Hom. ~~&~~ ~~Het~~het. nuc. in Fig. 2). Using the mass change as a metric for nucleation can be misleading as the number of hydrometeors produced can say more about the impact of the nucleation process than the mass change. ~~Another finding is the imbalance between condensation and evaporation. This indicates that evaporation, acting as a sink of liquid, is stronger than the source of liquid via condensation. This is likely a local feature as only the single column of Ny-Ålesund is used here. This feature indicates that the microphysical processes may also have a strong location dependency. For instance, in Ny-Ålesund, the air over the fjord is more moist than over the land (Kiszler et al., 2023), which may cause more evaporation over land if a cloud is advected there. Nevertheless, the message in Fig. 2 is clear that the phase changes between liquid and vapour, as well as frozen and vapour, dominate, while processes contributing to phase changes between liquid and frozen are not as relevant.~~ Evaluating this single column, shows that microphysical processes will depend on the chosen location although it became clear that the microphysical sinks found for liquid clouds is by far not as strong for mixed-phase and ice clouds. Especially, for the MPCs it became clear that the WBF process acts strongly upon the liquid mass and it is worth further investigating its behaviour.

3.2 ~~Regimes of phases~~

~~To get an overview of the cases used for the second part of the analysis, it isbeneficial to understand which temperature (T), vertical velocity (w), and ice/water saturation (S_i/S_w)regimes exist for the occurrence of the hydrometeors. These variables were chosen as the microphysical processes are directly connected to them~~

3.2 WBF in mixed-phase clouds

The Wegener-Bergeron-Findeisen process can be a reason why models have too little supercooled liquid, impacting the representation of MPCs. As shown in Kiszler et al. (2023) also in ICON-LEM, the amount of liquid-containing clouds is underestimated. In the previous section we have shown that the WBF process occurs very frequently in MPCs and could be a reason for the glaciation of these clouds. Therefore, this section aims to quantify and further explore the WBF process. The first investigated aspect is whether the evaporation rate would increase due to the WBF process. This does not necessarily have to be the case as evaporation could just occur more frequently but does not need to be stronger. To evaluate this aspect the subselection of MPCs was evaluated where evaporation was occurring (75 % of MPC cases). This set was split into two sets. The WBF set consists of cases where deposition occurs simultaneously and where it is, therefore, sub-saturated with respect to water and saturated with respect to ice. This makes up 42 % of the MPC cases. The other set consists of cases where no

~~Processes mean values and occurrence during the polar night (a) and polar day (b). Orange crosses and text indicate processes which affect the liquid phase, and purple dots and text those which affect the frozen phase.~~

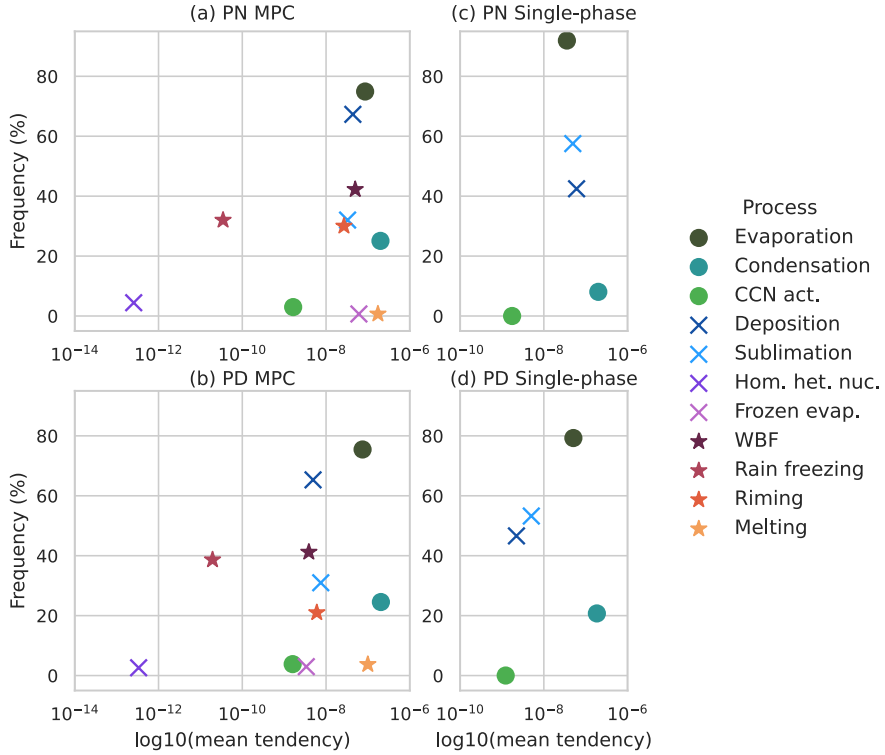

Figure 2. Microphysical processes mean tendencies and occurrence during the polar night (PN, a and c) and polar day (PD, b and d) shown for mixed-phase clouds (MPC, a and b) and for single-phase clouds (c and d). Dots indicate processes occurring between liquid water and vapour, crosses processes occurring between ice and vapour and stars processes between liquid water and ice.

deposition occurs (33 % of MPC cases). In Fig. 3 a), the distribution of the evaporation tendency for both evaporation sets is shown, and one can clearly see that they differ strongly. For the ~~analysis, we will exclusively consider grid points identified as cloudy.~~ WBF cases, the evaporation tendency is generally much larger than when no WBF is occurring. It should be kept in mind that this is a logarithmic scale, where two orders of magnitude make a large difference in the amount of liquid evaporating.

~~An overview of the distributions of the T, w and S_i for the polar night (PN) and polar day (PD)are given in Fig. 1. The polar night temperature ranges from -32 to 2 °C with the mean at -14 °C. In contrast, the warmer polar day varies less (-22 to 8 °C) and has a mean value of -2 °C. The vertical velocity is narrowly arranged around 0~~

Continuing with the impact on the total frozen and liquid mass, there too the question is whether the impact of the WBF process is significant or not. In Fig. 3 b) and c), one can see the distributions of frozen and liquid masses when deposition and no evaporation is occurring (no WBF, 25 ~~m s^{-1} for both polar night and day, and both the polar day and polar night low~~

variation (standard deviation: PD 0.35% of MPC cases) and when deposition and evaporation are occurring simultaneously (WBF, 42 m s^{-1}, PN 0.29% of MPC cases). Here, too, there are clear differences between the distributions, showing a shift towards higher frozen masses when WBF occurs. At the same time, the liquid mass distribution shifts towards lower values when WBF occurs. In Fig. 3 c), the tail of the liquid mass, which is visible for the cases where WBF occurs, is due to rain, which often occurs in subsaturated layers as it falls. Combined, this demonstrates visualizes the decrease in liquid mass while there is an increase in frozen mass when the WBF process occurs. For both Fig. 3 b) and c), we found the difference in the distributions to be statistically significant (Kruskal-Wallis test). This is also visible in the difference in mean values for both processes. When both processes occur at the same time, the average deposition rate experiences a fourfold increase ($9.8 \cdot 10^{-9}$ to $3.9 \cdot 10^{-8}$ m skg kg^{-1}). Extremes, which happen very rarely, are found more in the upwards motion, with the overall maximum at 6.43, while the average evaporation rate also increases by around one-order-of-magnitude ($2 \cdot 10^{-8}$ to $1.3 \cdot 10^{-7}$ m skg kg^{-1}. The saturation with respect to ice does not reach as high values during the polar day as during the polar night.). This shows that a significant amount of water transitions from liquid to vapour and then to the frozen phase via the WBF process.

Distribution of the temperature (a), vertical velocity (b) and ice saturation ratio (c) for the polar night (red) and polar day (blue).

As mentioned in Sec. 2.1, the hydrometeor types are split into frozen and liquid masses. Of the total 26.3 days of low-level clouds during the polar night, almost all contain periods with frozen hydrometeors (25.4 days), Several other interesting findings appeared when we looked into the question where and under what circumstances the WBF process occurs. There we looked into the temperature distribution of the WBF process and found that the WBF process seems to correlate more strongly with deposition than with evaporation (Fig. 4). Additionally, one can see that the distributions look different between the PN and PD (Fig. 4 a and b respectively). While during the PN the WBF process most frequently occurs between -6 and slightly more than half contain liquid hydrometeors (15.5 days, 58-13 %). For the 37.9 days of low-level clouds during the polar day, almost all times contained liquid (96°C, during the PD two maxima are visible one around -3 %) while only 31°C and one around -10 % contained ice. This is connected to the fact that liquid occurs °C. As deposition should decrease with increasing temperature the peak at higher temperatures , which are more prevalent during the polar day was not expected. Therefore, we investigated whether other processes could be influencing this. Indeed, it seems like riming and rain freezing play a role in the deposition and WBF rate increase during the PD at higher temperatures (Fig. 1 a). To put the process rates into context, the liquid and frozen mass mixing ratios themselves generally lie between 10^{-8} and 10^{-3} kg4 b). We hypothesize that the increase is due to the fact, that both riming and rain freezing increase the ice mass creating more frozen mass on which vapour may deposit. This would explain the increase of the deposition rate above -5 kg−1. Another aspect to note is that similar to Shupe et al. (2008) and as theorized by Korolev (2008), °C causing the WBF process to set in.

Another aspect which we evaluated was whether the deposition rate or the evaporation rate is the limiting factor for the WBF rate, as the WBF rate is based on the minimum rate of both. To explore this we used the supercooled liquid fraction

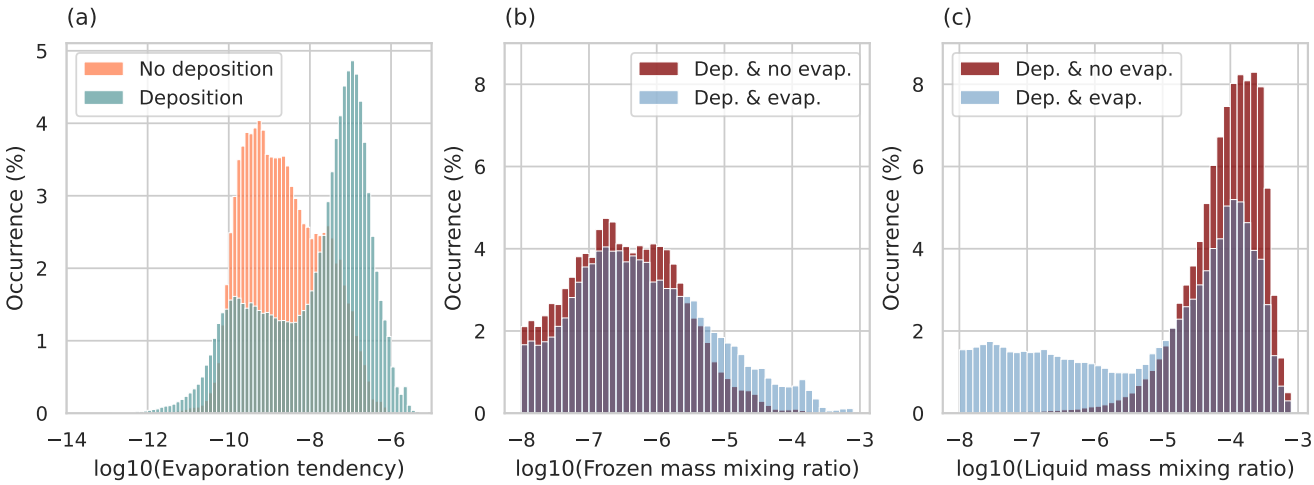

Figure 3. Histograms of the logarithm of evaporation tendency (a), frozen mass (b) and liquid mass (c). a) Liquid mass change due to evaporation in each timestep (evaporation tendency) for MPCs where no deposition occurs (orange, 33 %) and where deposition occurs (green, 42 %). b) Frozen mass for MPCs where deposition but no evaporation occurs (red, 25 %) and where deposition and evaporation occur simultaneously (blue, 42 %). c) is analogue to b) but shows the liquid mass.

(SLF, Komurcu et al., 2014) to categorize the clouds. An SLF of 1 indicates a pure liquid cloud and 0 a pure ice cloud. A mixed-phase cloud would lie between 0 and 1. Using the SLF we found that ~~higher upward vertical velocities are connected to higher saturation and with that also to higher hydrometeor masses (not shown). This already hints towards potential correlations between certain processes and the vertical wind and saturation~~there seem to be two WBF regimes, one for clouds with high liquid amount and one for clouds with low liquid content. In cases where the liquid mass dominates, deposition is the limiting factor for the WBF process while for low liquid mass, evaporation limits the WBF rate. This is understandable if one considers that if there is less ice available the deposition rate will be lower and if there is less liquid available there will be less mass available to evaporate (see Fig. B1 for a visualization).

3.3 Dependence on environmental conditions

~~An interesting aspect of~~ Looking at the WBF process, and the difference of processes between PN and PD indicates that thermodynamic conditions influence the microphysical processes~~is the circumstances under which they occur~~. To understand more about ~~this, the temperature, w, S_i and S_w were used to evaluate the processes in different regimes~~these dependencies, the microphysical processes behaviours with temperature, vertical velocity and saturation (ice, liquid water) were evaluated. It is worth mentioning here that sublimation and deposition can not occur at the same time as they are calculated by the same process. The same is true for evaporation and condensation. Other processes can occur at the same time.

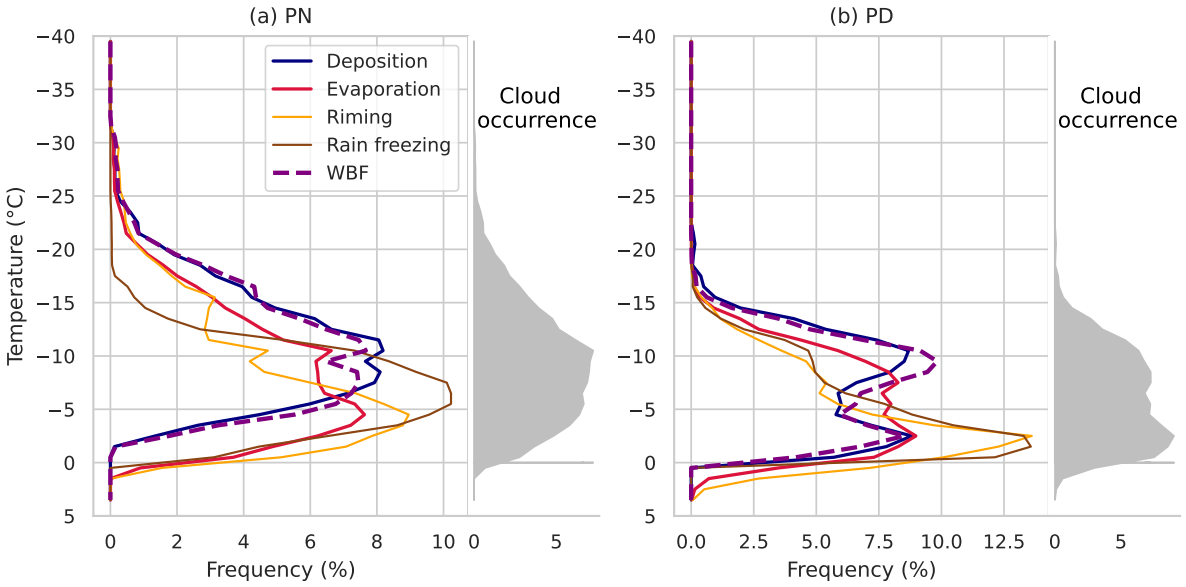

Figure 4. Occurrence frequency of microphysical processes with temperature shown for the polar night (PN, a) and the polar day (PD, b). Microphysical processes shown are deposition (blue), evaporation (red), WBF (purple, dashed), riming (yellow) and rain freezing (brown). The distribution of the mixed-phase clouds are shown in grey for both PN and PD.

Starting with the ~~processes affecting the frozen mass and the temperature~~ temperature dependency, it can be seen that deposition ~~and sublimation occur~~ occurs relatively consistently at all temperatures below 0 °C (Fig. 5 ~~i and j~~ f) while the mean mass change decreases (Fig. 5 ~~c and d). For sublimation the tendency spread also increases with temperature, which cannot be seen as clearly for deposition~~ b). Sublimation shows a similar behaviour (appendix Fig. C1 a and f), although deposition shows a slight maximum between around -10 and -20 °C where sublimation has a minimum. Another process showing a decreasing tendency with temperature is rain freezing, which occurs more often for higher temperatures, but the amount of frozen mass ~~increases~~ decreases with temperature (5 ~~f and l~~e and j). Rain freezing, as expected, is more efficient ~~with~~ at lower temperatures but has less total impact the colder it is. Interestingly, a bi-modal distribution is visible in Fig. 5 ~~c and k~~ d and i for riming for both the tendency as well as the occurrence. One ~~maxima lies below approx.~~ maximum lies below approximately -20 °C, where there are altogether few cases, and one above -10 °C. This is possibly connected to the maximum saturation difference between ice and liquid water as the cloud droplet mean mass has a local minimum of around -18 °C. This hypothesis would be supported by the maximum of deposition in regions where riming is lowest.

Of the processes affecting the liquid mass, evaporation dominates throughout all temperature ranges where liquid occurs. Both the occurrence and the tendency of evaporation increase with increasing temperatures (Fig. 5 b and g). Of all processes, evaporation shows the largest tendency spread which potentially indicates that it may be more strongly influenced by other

factors for negative temperatures, than other processes which depend more clearly on the temperature. Combining the evaporation and deposition, the WBF process occurrence has a clear maximum between -10 and -5 °C (Fig. 5 h). At the same time WBF seems to have the highest tendency for values below -20 °C, although here again caution is required due to the number of cases (Fig. 5 c).

Further processes, shown in the appendix, include condensation, which has a relatively constant tendency and increases with temperature in occurrence, and CCN activation which occurs rarely and its occurrence with temperature is similar to condensation (Fig. C1). Melting and evaporation, due to melting, are only active above 0 °C and decrease accordingly with increasing temperatures as less and less frozen mass is available ~~. The homogeneous~~ (Fig. C1). Homogeneous and heterogeneous ice nucleation ~~and cloud droplet homogeneous freezing happen so rarely that they are not further included. CCN activation occurs throughout all temperatures above -34 °C but is likewise seldom, especially below -20 °C. The main processes affecting the liquid mass, as discussed above, are the processes of phase change, which affect the frozen mass, evaporation, and condensation. It is intriguing that evaporation appears to be the most prominent process throughout all temperature regimes~~ occurs very rarely and more cases would be required to properly describe its thermodynamic dependencies (Fig. ~~5), with condensation being less prominent. On the other hand, condensation has, on average, a higher mean mass change and shows much less spread consistently throughout all temperature bins~~C1).

The next variable to look at is the vertical velocity. ~~For the frozen mass, only three processes showed a signal ; therefore, this section will focus on those. One~~ This section only focuses on processes where a signal can be seen. One process is riming, which increases with upward velocity in occurrence. This can mainly be seen during the ~~polar night~~ PN as riming is much more frequent there (Fig. 6 b). The riming tendency may suggest an increase with upwards velocity as shown in Fig. 6 a), although the fact that only 1 % of the cases are above 1.2 m s^{-1} makes this slightly speculative. If one discards the lowest and highest 1 % of the vertical wind speed, then the decrease of sublimation with upward velocity and its ~~increases~~ increase towards higher downward velocity can be seen (Fig. 7 a, white areas.). For sublimation, no difference in the behaviour between polar night and day is found. For deposition, one would expect the opposite behaviour, but as visible in 7 b), combining the ~~polar day and polar night~~PD and PN, such behaviour is not completely obvious.

Interestingly, for deposition, a difference in its behaviour with ~~*w*~~ vertical velocity can be seen between ~~polar night and polar day~~PN and PD. The deposition frequency increases with upward velocity clearly for the ~~polar night~~ PN (Fig. 7 c). This behaviour is not so clear for the ~~polar day~~ PD(Fig. 7 d), where deposition seems common for downward motion. Additionally, the deposition rate during PD does not show a strong dependence on the vertical velocity (not shown), although previous observations show a decrease of ice mass with downward motion (Shupe et al., 2008)~~. Reasons for this behaviour~~ , suggesting potentially less deposition. To add to the discussion, the WBF occurrence with vertical velocity, shows a similar signal as the deposition for the PN and PD (Fig. 7). Even though the WBF is computed from the evaporation and deposition, the evaporation occurrence does not seem to vary strongly with the velocity (Fig. C2). In addition, we found that condensation consistently

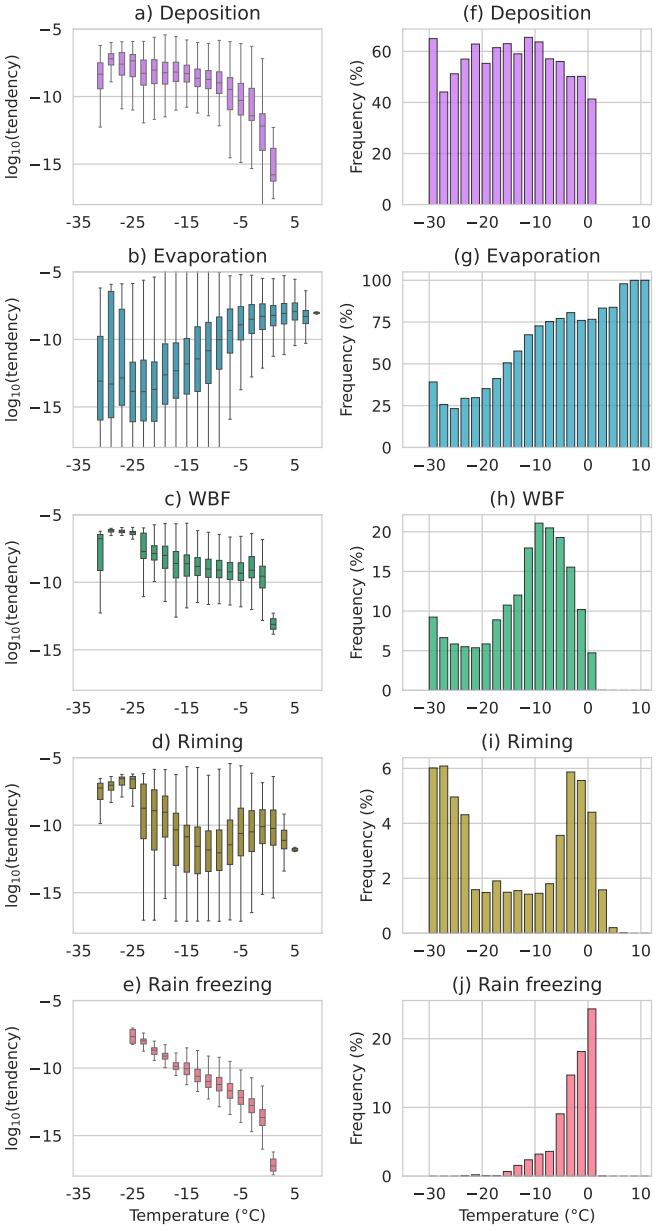

Figure 5. Temperature dependence of microphysical processes. Left column: box plots for temperature bins. Right column: ~~Occurrence~~ occurrence for each temperature bin. The data includes the polar night and polar day, and bins of 2 °C are used.

increases for PN and PD towards upwards velocities, as one would expect (Fig. C2). As theorized by Korolev (2008) the WBF process is to a certain extent expected for downwards velocities, which can explain some of the behaviour of the deposition tendency during the PD. At the same time, it is expected that for upwards velocities saturation with respect to ice and water will set in, causing condensation to increase and therefore preventing the WBF process. This is we only found partially.

Reasons for the behaviours of the WBF process and deposition could be the lower number of frozen cases during PD or the differences in temperature range. Another reason could be differences in the vertical structure of the boundary layer and potentially increased moisture in the lower layers due to the fjord by Ny-~~Å~~Ålesund. One must keep in mind that the vertical wind is very narrowly distributed around 0 m s^{-1}, and only a few absolute high values exist. To study this further, other types of clouds that have stronger vertical velocities by nature are more suitable. For the liquid mass, similarities exist between evaporation and sublimation, as both show a decrease with upward velocity. Condensation resembles the deposition more strongly and increases with upward motion. The CCN activation is, by definition, dependent on the vertical velocity. Therefore, the increase with higher upward velocity, which we found, is as expected.

The ~~next aspect~~ last thermodynamic variable is the saturation with respect to ice and water. Processes that change the frozen mass are evaluated against ~~S_i~~ the saturation with respect to ice. Here, riming stood out again. It can be seen in Fig. 6 c and d that riming increases with saturation in both occurrence and mean tendency. This fits the increase of riming, which was described for higher upward velocities as the saturation of the rising air can increase. Some processes depend, by definition, on the saturation, for instance, deposition/sublimation and condensation/evaporation. The signal found for these processes ~~showed~~ indicated evaporation and sublimation below saturation and condensation and deposition above saturation, which was, therefore, expected (not shown). What was noticeable, though, was that the tendency of condensation showed a higher mean in combination with a much smaller spread in comparison to evaporation. It was generally an interesting finding that some processes, such as condensation and rain freezing, showed much less spread in their tendency than others ~~.~~

3.4 ~~WBF in mixed-phase clouds~~

~~The introduction mentions that the Wegener-Bergeron-Findeisen process can be a reason why models have too little supercooled liquid, impacting the representation of MPCs. As shown in Kiszler et al. (2023) also in ICON-LEM, the amount of liquid-containing clouds is underestimated. Therefore, we want to go beyond evaluating single processes and demonstrate, using the WBF process, how the process rates tell us more about intertwined processes in clouds. In the previous sections, it became clear that evaporation occurs frequently. The hypothesis is that this evaporation could partially be increased as part of the WBF process. This could suppress the production of liquid in the first place or decrease the amount of liquid in a mixed-phase cloud. To see if the WBF process can be found for the data in this study, a subset containing only mixed-phase clouds was produced (frozen mass and liquid mass both above 10^{-8} kg kg^{-1}). Then, all points where evaporation occurred were selected and split into two sets. One has cases where deposition occurs simultaneously and where it is, therefore, sub-saturated with respect to water and saturated with respect to ice. The other set has cases where no deposition occurs.~~

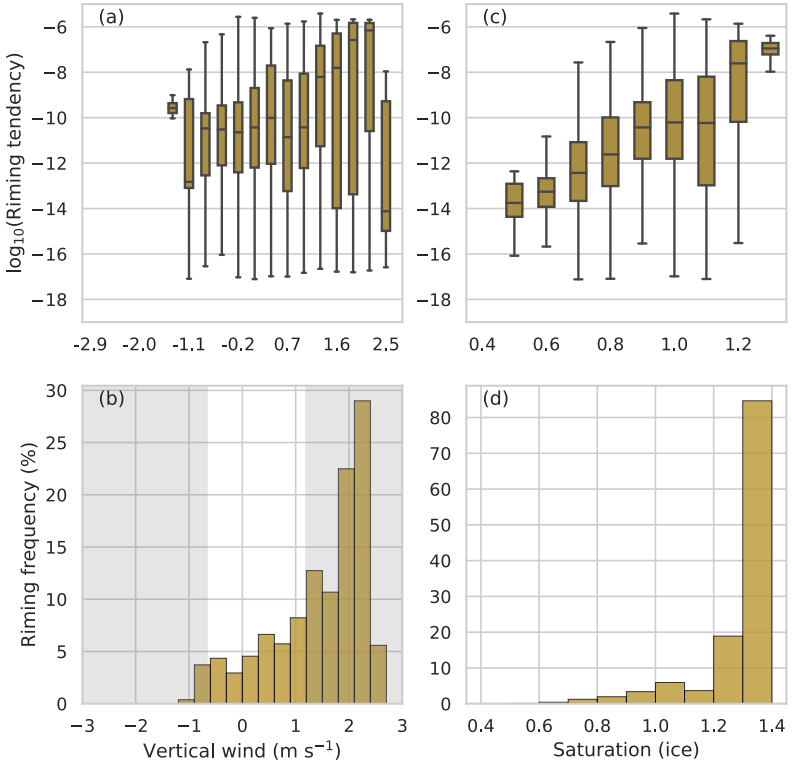

Figure 6. Dependence of riming on the vertical wind speed (left column) and the saturation with respect to ice (right column) for the polar night. The upper rows show the distribution of the riming tendency per bin as boxplots. The lower row shows the frequency of occurrence per bin. Bins of 0.1 are used for the saturation and 0.3 m s^{-1} for the vertical wind. The grey shaded areas indicate each the lowest and highest 1 % vertical wind speeds.

~~In Fig. 3 a), the distribution of the evaporation tendency for both evaporation sets is shown, and one can clearly see that they differ strongly. For the cases where deposition is happening at the same time as evaporation, the evaporation tendency is generally much larger than when no deposition is occurring. It should be kept in mind that this is a logarithmic scale, where two orders of magnitude make a large difference in the amount of liquid evaporating. In Fig. 3 b) and c), one can see the distributions of frozen and liquid masses when deposition and no evaporation is occurring and when deposition and evaporation are occurring simultaneously. Here, too, there are clear differences between the distributions, showing a shift towards higher frozen masses when deposition and evaporation occur at the same time. At the same time, the liquid mass distribution shifts towards lower values when both processes occur. In Fig. 3 c), the tail of the liquid mass, which is visible for the deposition and evaporation cases, is due to rain, which often occurs in subsaturated layers as it falls. Combined, this demonstrates a decrease in liquid mass while there is an increase in frozen mass for cases where deposition and evaporation occur at the same time. For both Fig. 3 b) and c), we found the difference in the distributions to be statistically significant. This is also visible in the difference in mean values for both processes. When both processes occur at the same time, the average deposition~~

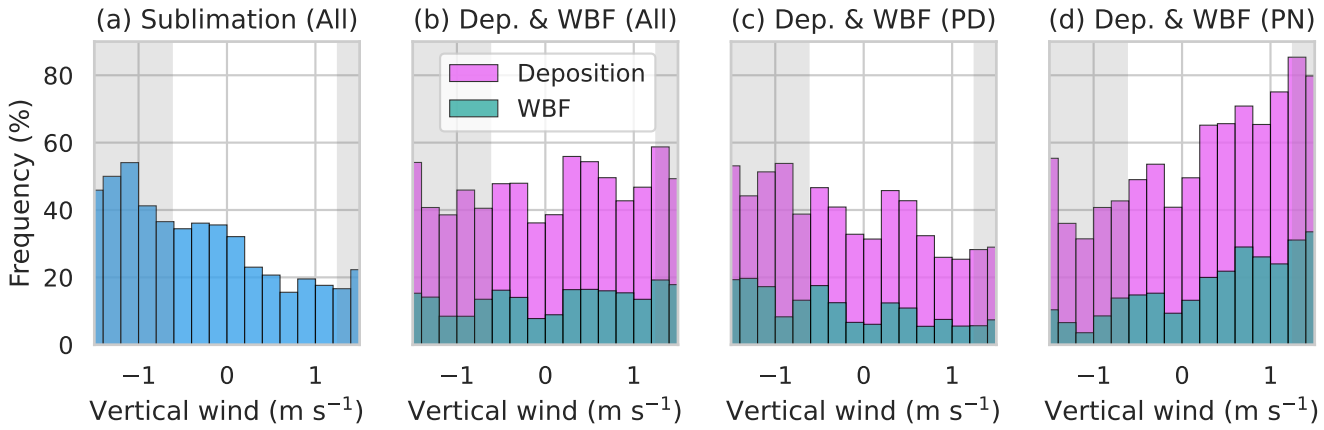

Figure 7. Occurrence of sublimation (a) and deposition and WBF (b-d) with vertical velocity (bin width: ~~0.3~~ 0.2 m s^{-1}). Sublimation is shown for ~~polar day~~ PD and ~~night~~ PN (a), deposition and WBF for ~~polar day~~ PD and ~~night~~ PN (b), the ~~polar day~~ PD (c), and ~~polar night~~ PN (d). The grey boxes mark the lowest and highest 1 % of the vertical wind.

~~rate experiences a one-order-of-magnitude increase ($9.8 \cdot 10^{-9}$ to $3.9 \cdot 10^{-8}$ kg kg^{-1}), while the average evaporation rate also increases with the same order of magnitude ($2 \cdot 10^{-8}$~~ in respect to ~~$1.3 \cdot 10^{-7}$ kg kg^{-1}). This suggests that a significant amount of water transitions from liquid to vapour and then to the frozen phase via the WBF process. It would be interesting to explore the sensitivity of the WBF process to changes in the process rates further. Such analysis is beyond the scope of this study, but it is worth noting that the developed methods are readily usable to perform such sensitivity studies~~all thermodynamic variables evaluated here.

~~Histograms of the logarithm of evaporation tendency (a), frozen mass (b) and liquid mass (c). a) Liquid mass change due to evaporation in each timestep (evaporation tendency) for MPCs where no deposition occurs (orange) and where deposition occurs (green). b) Frozen mass for MPCs where deposition but no evaporation occurs (red) and where deposition and evaporation occur simultaneously (blue). c) is analogue to b) but shows the liquid mass.~~

4 Discussion and conclusions

This study evaluates the microphysical processes of the two-moment microphysics scheme from Seifert and Beheng (2006) as it is implemented in ICON. The area of focus is Svalbard, and only low-level clouds are selected for the analysis. A further separation is made between single-phase and mixed-phase clouds. Using a wrapper to run the microphysics scheme offline as a diagnostic tool, the process rates per timestep are written out. In total, eight months, four polar night and four polar day, are simulated. The goal is to determine which processes play the largest role in the phase transitions in Arctic low-level clouds and in what way they depend on temperature, vertical velocity and saturation.

It was found that the dominating processes are phase transitions between liquid hydrometeors and vapour, as well as frozen hydrometeors and vapour. The results suggest one possible approach to improving the representation of the phase-partitioning in low-level mixed-phase clouds in the Arctic could be to adjust the processes of evaporation/condensation and deposition/-sublimation. Another approach could be to increase the activity of processes which are currently less active, as these may not be active enough. Further, the differences between polar night and polar day showed the importance of evaluating a large dataset covering different thermodynamic conditions. For instance, rain freezing ~~impacted the frozen mass~~ seemed to be more important during the polar day ~~much more~~ than during the polar night, while riming seemed to be more important during polar night. It is worth mentioning that nucleation processes only minimally change the mass directly, but the numbers of activated CCN and INP have an impact on other process rates. Fan et al. (2017) showed this in a case study for orographic clouds where evaporation became stronger than condensation for higher aerosol concentrations, whereas for lower concentrations, the process rates were similar. Therefore, although changes to evaporation/condensation and deposition/sublimation likely will cause large hydrometeor mass changes, the interaction between processes also plays an important role.

When combining the deposition and evaporation tendency it became clear that the Wegener-Bergeron-Findeisen process, where liquid water evaporates and then deposits on ice due to the lower saturation of ice below 0°C, also plays an important role. Using the minimum of evaporation and deposition, when they occur simultaneaously, we computed an approximate WBF tendency. We found a very frequent occurrence of 42 % of the WBF process in MPCs. Further, it seems like the deposition tendency drives the occurrence of the WBF process. Additionally, the evaporation tendency was evaluated in combination with the frozen and liquid mass. This showed a one-order-of-magnitude increase of the average evaporation, causing a significant decrease of the liquid mass. Combined, the results showed that a significant amount of mass follows the WBF pathway from liquid to vapour to the frozen phase with an average WBF tendency similar to the average deposition tendency. Reducing the WBF rate by reducing the deposition tendency may be a way to reduce the underestimation of liquid-containing clouds found in a previous study (Kiszler et al., 2023).

We further explored how each process behaves in different thermodynamical regimes. Temperature is one important factor that determines the importance of a process. For instance, Fan et al. (2017) found that for warm orographic ~~MPC~~ MPCs riming was similarly important for the snow formation as deposition, but for cold orographic ~~MPC~~ MPCs deposition was clearly more important. In this study, differences are visible between the polar night and day. We found that melting and rain freezing play a larger role during the polar day while riming decreases in importance during that time. This dependence on temperature was further evaluated, and it could be seen that processes that change the mass phase between liquid and frozen show a stronger temperature dependence than those involving vapour phase transitions. The strongest temperature dependence was visible for rain freezing, which showed an increasing occurrence with increasing temperatures, while the mean frozen rain mass decreased. Interestingly, the distribution of riming for both occurrence and mean mass change in different temperature regimes was ~~bimodal~~bi-modal, showing a minimum between -20 and -10 °C. The connections between the process rates and the vapour saturation and vertical wind were not as clear. This can partially be attributed to the narrow range of values for these

thermodynamic variables given in low-level Arctic clouds. The clearest signal, in this respect, was the increase of riming with increasing upward velocities. This could be connected to the larger production of liquid in updrafts where ~~the WBF process is not active (Ervens et al., 2011; Korolev, 2008).~~

~~Going a step beyond single process rates, we demonstrated how the combination of process rates can teach us more about intertwined processes. Here, we looked at the Wegener-Bergeron-Findeisen process, where liquid water evaporates and then deposits on ice due to the lower saturation of ice below 0°C. For this purpose, only mixed-phase clouds were selected. The evaporation tendency was evaluated in combination with the frozen and liquid mass, and the results suggest that a notable amount of mass follows the WBF pathway from liquid to vapour to the frozen phase. Reducing this amount may be a way to reduce the underestimation of liquid-containing clouds found in a previous study (Kiszler et al., 2023)~~condensation is more active. Another finding was that the WBF process did not fully behave with vertical velocity as one may expect it from the theoretical understanding Korolev (2008). We found that for upwards velocities the WBF process seems to increase is activity during the PN.

As stated above, there are limitations to our approach, which might make it less insightful for cases where advection dominates the cloud hydrometeor composition, for instance, in deep convective cases. Nevertheless, when focusing on low-level clouds in the Arctic, this approach provides valuable insights in regard to the processes inside the clouds, as demonstrated in this study. Additionally, the regimes of vertical velocity and temperatures studied here are limited to those of low-level clouds in the Arctic. Specifically over Ny-Ålesund which, as we found, represents more the decaying phase of clouds than the formation phase. Therefore, to create a broader picture of the microphysical processes in other cloud types, further studies, including stronger vertical velocities and larger temperature ranges, are necessary. This could, for instance, substantiate our findings in regard to the increase of riming with higher upward vertical velocities.

There are further factors that impact the process rates, as mentioned in the introduction. These include aerosol concentrations, which can strongly impact the hydrometeor composition and cloud lifetime (Kalesse et al., 2016; Eirund et al., 2019). In this study, the CCN and INP are treated as maritime, which is more accurate than the default continental setting in ICON but still not completely correct. CCNs and INPs are another large area of active research, which is why this study focuses on the processes independently of aerosol influences. An interesting study would be, though, how tweaked CCN and IN settings impact the process rates using the approach presented here. Using the process rates and looking into the regimes where different processes occur has shown that this method is also valuable for studying individual processes in greater depth. Being able to quickly change a process setting and get an idea of what might change in the model has proven easy and reliable. This encourages continuing to use tools such as this wrapper, which simplifies the untangling of complex cloud microphysics schemes.

Code and data availability. The microphysical wrapper code is stored on the DKRZ Gitlab. In the form used here, the wrapper includes ICON code which is licensed and the code is therefore only available on request. The ICON model code which we used is available for

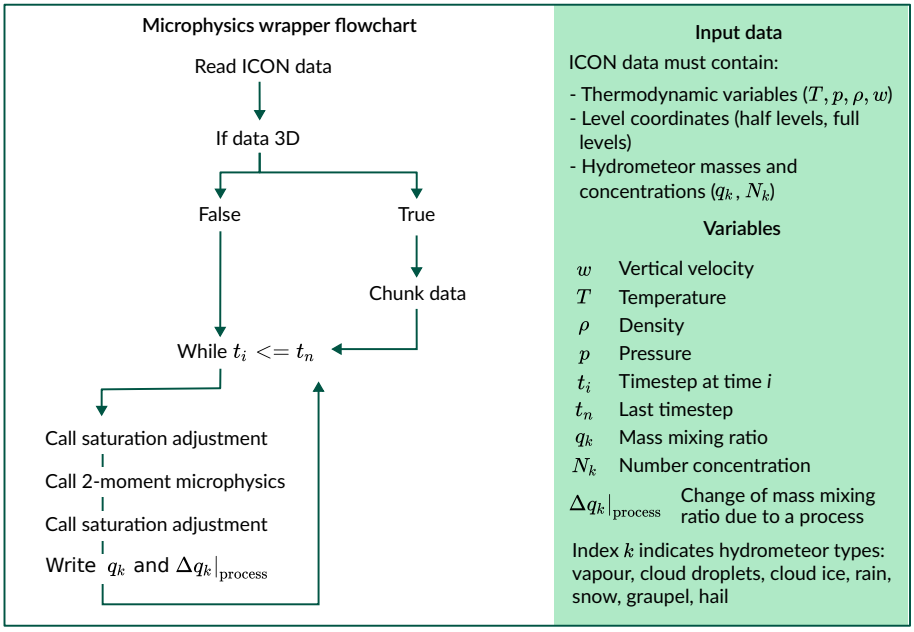

Figure A1. Flowchart illustrating the microphysical parameterisation wrapper. The variables and required input data are listed on the right. Any sub-selection of the data was done after running the wrapper. Each process has a separate tendency for each hydrometeor which it affects ($\Delta q_k|_{\text{process}}$).

institutions or individuals under a licence but a recently published open source version is available here: https://icon-model.org/. The process rates, low-level cloud selection and meteograms are available on Zenodo with the DOI: 10.5281/zenodo.10117706. A GitHub repository containing the code necessary to reproduce the results can be found here: 10.5281/zenodo.10945484

Appendix A: Flowchart of microphysical wrapper

Appendix B: WBF dependence on SLF

The supercooled liquid fraction (SLF) is computed based on (Komurcu et al., 2014).

$$SLF = \frac{r_{\text{liquid water}}}{r_{\text{liquid water}} + r_{\text{ice}}}$$

In Fig. B1 three different microphysical processes are shown: deposition, evaporation and WBF. The SLF generally has two maxima in occurrence towards 0 and 1. This figure demonstrates how the WBF process is limited by deposition for high SLF and by evaporation in low SLF regimes.

Appendix C: Processes dependence on environmental conditions

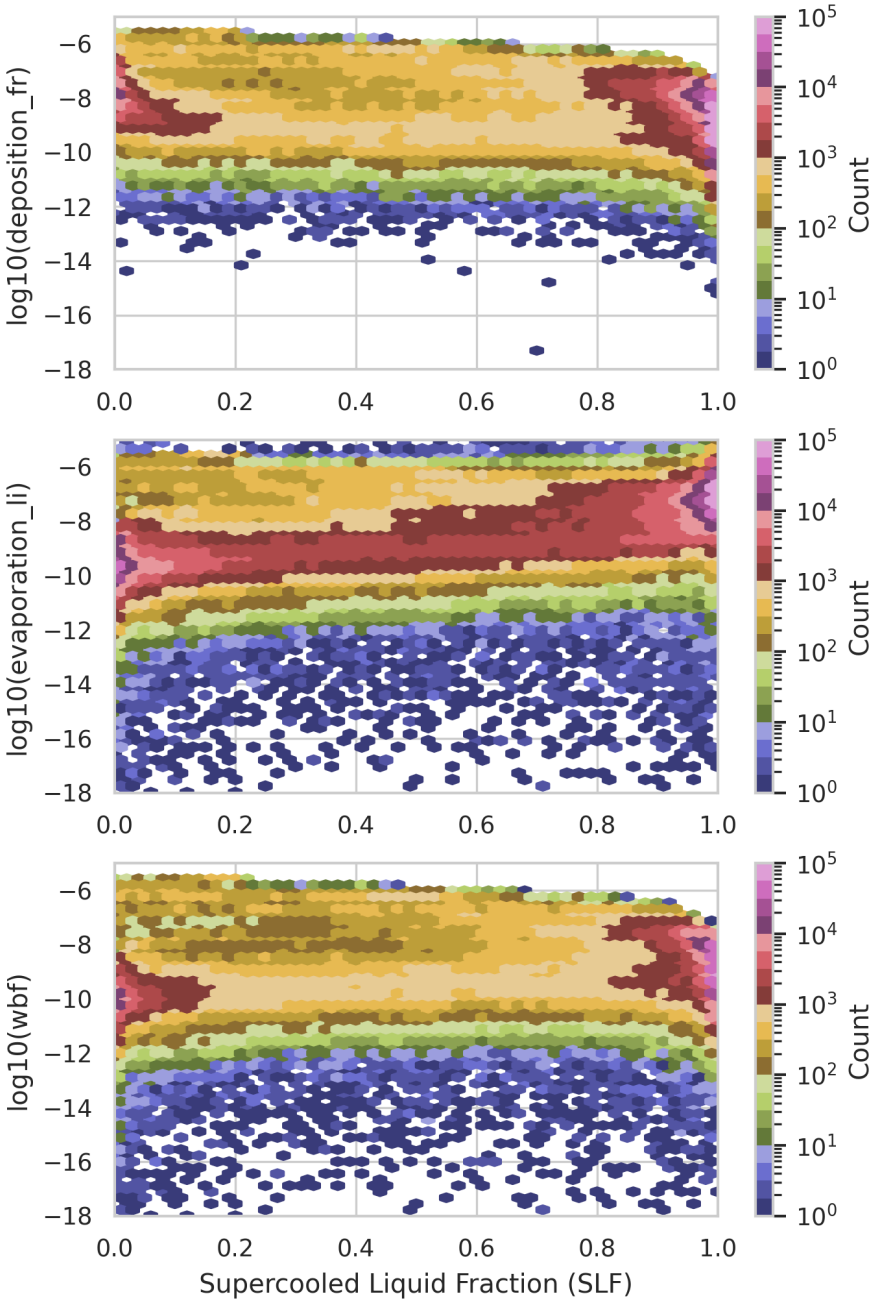

Figure B1. 2D-histograms demonstrating the connection between clouds with high SLF and low SLF and the microphysical processes: a) deposition, b) evaporation and c) WBF. The colourbars indicate the count of the cases.

This section provides additional figures for the dependence of the microphysical processes on the temperature, vertical velocity and saturation. They are complementary to the figures shown in section 3.3 and just show additional processes mentioned in the results.

Author contributions. TK carried out the wrapper implementation, data processing, and method development, created the visualisations and prepared the manuscript with contributions from all co-authors. VS and DO contributed to the conceptualisation, research supervision, and discussion of results.

Competing interests. The authors declare that no competing interests are present.

Acknowledgements. We gratefully acknowledge the funding by the Deutsche Forschungsgemeinschaft (DFG, German Research Foundation) – Project number 268020496 – TRR 172, within the Transregional Collaborative Research Center "ArctiC Amplification: Climate Relevant Atmospheric and SurfaCe Processes, and Feedback Mechanisms (AC)3. This work used resources of the Deutsches Klimarechenzentrum (DKRZ) granted by its Scientific Steering Committee (WLA) under project ID bb1086. We thank Axel Seifert for the support in implementing the microphysics wrapper. Further, the discussions with Rosa Gierens, Giovanni Chellini and Matthew Shupe helped shape the analysis. Two anonymous reviewers additionally helped to improve this manuscript, which we are grateful for.

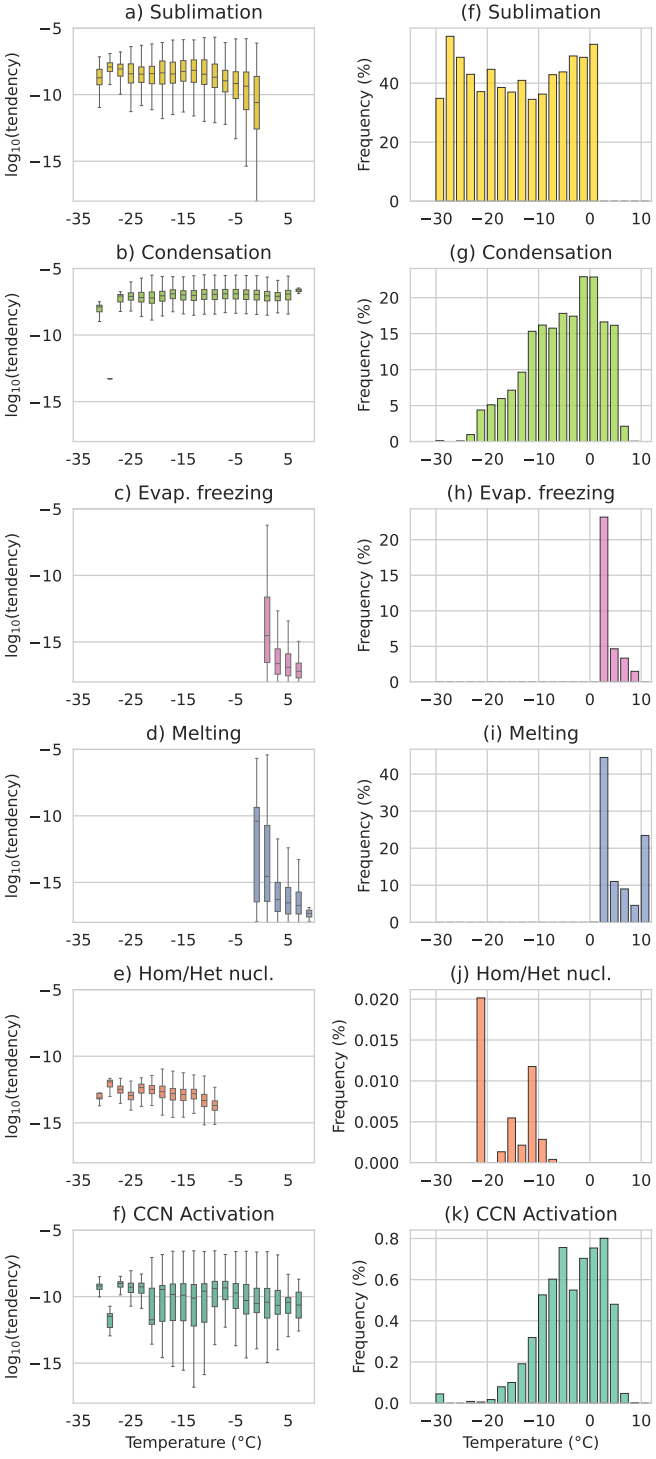

Figure C1. Temperature dependence of microphysical processes. Left column: box plots for temperature bins. Right column: occurrence for each temperature bin. The data includes the polar night and polar day, and bins of 2 °C are used.

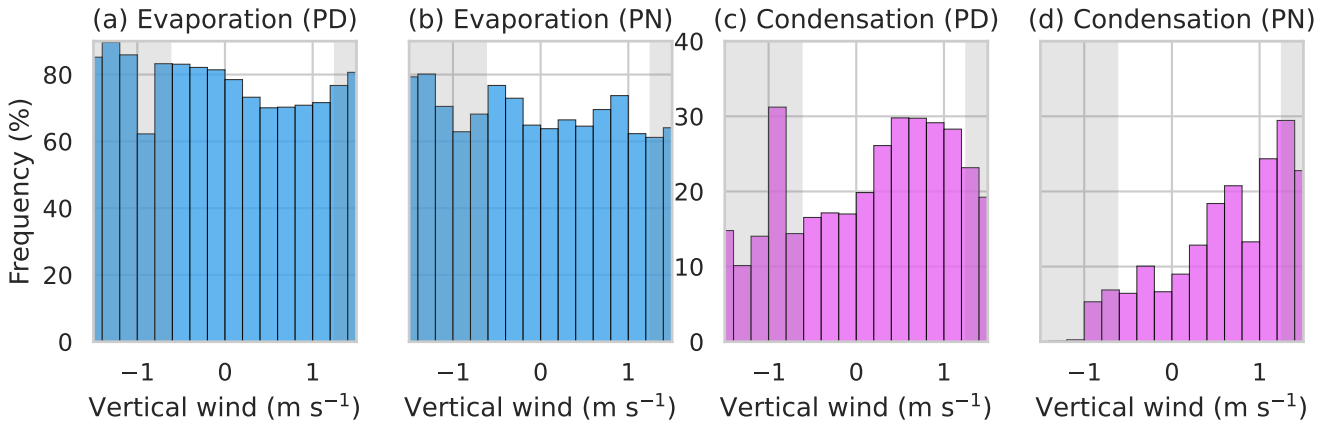

Figure C2. Dependence of evaporation (a and b) and condensation (c and d) on the vertical velocity. Split into PD (a and c) and PN (b and d) using 0.2 m s^{-1} bins.

References

Barrett, A. I. and Hoose, C.: Microphysical Pathways Active within Thunderstorms and Their Sensitivity to CCN Concentration and Wind Shear, Journal of Geophysical Research: Atmospheres, p. e2022JD036965, https://doi.org/https://doi.org/10.1029/2022JD036965, e2022JD036965 2022JD036965, 2023.

Blahak, U.: Towards a Better Representation of High Density Ice Particles in a State-of-the-Art Two-Moment Bulk Microphysical Scheme, in: 15 th International Conference on Clouds and Precipitation, 2008.

Cesana, G. and Chepfer, H.: How well do climate models simulate cloud vertical structure? A comparison between CALIPSO-GOCCP satellite observations and CMIP5 models, Geophysical Research Letters, 39, https://doi.org/https://doi.org/10.1029/2012GL053153, 2012.

Chellini, G., Gierens, R., and Kneifel, S.: Ice Aggregation in Low-Level Mixed-Phase Clouds at a High Arctic Site: Enhanced by Dendritic Growth and Absent Close to the Melting Level, Journal of Geophysical Research: Atmospheres, 127, e2022JD036 860, https://doi.org/https://doi.org/10.1029/2022JD036860, e2022JD036860 2022JD036860, 2022.

Curry, J. A. and Ebert, E. E.: Annual Cycle of Radiation Fluxes over the Arctic Ocean: Sensitivity to Cloud Optical Properties, Journal of Climate, 5, 1267 – 1280, https://doi.org/https://doi.org/10.1175/1520-0442(1992)005<1267:ACORFO>2.0.CO;2, 1992.

Dipankar, A., Stevens, B., Heinze, R., Moseley, C., Zängl, G., Giorgetta, M., and Brdar, S.: Large eddy simulation using the general circulation model ICON, Journal of Advances in Modeling Earth Systems, 7, 963–986, https://doi.org/10.1002/2015MS000431, 2015.

Ebell, K., Nomokonova, T., Maturilli, M., and Ritter, C.: Radiative Effect of Clouds at Ny-Ålesund, Svalbard, as Inferred from Ground-Based Remote Sensing Observations, Journal of Applied Meteorology and Climatology, 59, 3 – 22, https://doi.org/https://doi.org/10.1175/JAMC-D-19-0080.1, 2020.

Eirund, G. K., Possner, A., and Lohmann, U.: Response of Arctic mixed-phase clouds to aerosol perturbations under different surface forcings, Atmospheric Chemistry and Physics, 19, 9847–9864, https://doi.org/10.5194/acp-19-9847-2019, 2019.

Ervens, B., Feingold, G., Sulia, K., and Harrington, J.: The impact of microphysical parameters, ice nucleation mode, and habit growth on the ice/liquid partitioning in mixed-phase Arctic clouds, Journal of Geophysical Research: Atmospheres, 116, https://doi.org/https://doi.org/10.1029/2011JD015729, 2011.

Fan, J., Leung, L. R., Rosenfeld, D., and DeMott, P. J.: Effects of cloud condensation nuclei and ice nucleating particles on precipitation processes and supercooled liquid in mixed-phase orographic clouds, Atmospheric Chemistry and Physics, 17, 1017–1035, https://doi.org/10.5194/acp-17-1017-2017, 2017.

Gettelman, A. and Morrison, H.: Advanced Two-Moment Bulk Microphysics for Global Models. Part I: Off-Line Tests and Comparison with Other Schemes, Journal of Climate, 28, 1268 – 1287, https://doi.org/https://doi.org/10.1175/JCLI-D-14-00102.1, 2015.

Gettelman, A., Morrison, H., Terai, C. R., and Wood, R.: Microphysical process rates and global aerosol–cloud interactions, Atmospheric Chemistry and Physics, 13, 9855–9867, https://doi.org/10.5194/acp-13-9855-2013, 2013.

Gierens, R., Kneifel, S., Shupe, M. D., Ebell, K., Maturilli, M., and Löhnert, U.: Low-level mixed-phase clouds in a complex Arctic environment, Atmospheric Chemistry and Physics, 20, 3459–3481, https://doi.org/10.5194/acp-20-3459-2020, 2020.

Goosse, H., Kay, J. E., Armour, K. C., Bodas-Salcedo, A., Chepfer, H., Docquier, D., Jonko, A., Kushner, P. J., Lecomte, O., Massonnet, F., Park, H.-S., Pithan, F., Svensson, G., and Vancoppenolle, M.: Quantifying climate feedbacks in polar regions, Nature Communications, 9, 1919, https://doi.org/10.1038/s41467-018-04173-0, 2018.

Heinze, R., Dipankar, A., Henken, C. C., Moseley, C., Sourdeval, O., Trömel, S., Xie, X., Adamidis, P., Ament, F., Baars, H., Barthlott, C., Behrendt, A., Blahak, U., Bley, S., Brdar, S., Brueck, M., Crewell, S., Deneke, H., Girolamo, P. D., Evaristo, R., Fischer, J., Frank, C., Friederichs, P., Göcke, T., Gorges, K., Hande, L., Hanke, M., Hansen, A., Hege, H., Hoose, C., Jahns, T., Kalthoff, N., Klocke, D., Kneifel, S., Knippertz, P., Kuhn, A., Laar, T. v., Macke, A., Maurer, V., Mayer, B., Meyer, C. I., Muppa, S. K., Neggers, R. A. J., Orlandi, E., Pantillon, F., Pospichal, B., Röber, N., Scheck, L., Seifert, A., Seifert, P., Senf, F., Siligam, P., Simmer, C., Steinke, S., Stevens, B., Wapler, K., Weniger, M., Wulfmeyer, V., Zängl, G., Zhang, D., and Quaas, J.: Large-eddy simulations over Germany using ICON: a comprehensive evaluation, Quarterly Journal of the Royal Meteorological Society, 143, 69–100, https://doi.org/10.1002/qj.2947, 2017.

Huang, Y., Dong, X., Kay, J. E., Xi, B., and McIlhattan, E. A.: The climate response to increased cloud liquid water over the Arctic in CESM1: a sensitivity study of Wegener-Bergeron-Findeisen process, Climate Dynamics, 56, 3373–3394, https://doi.org/10.1007/s00382-021-05648-5, 2021.

Kalesse, H., de Boer, G., Solomon, A., Oue, M., Ahlgrimm, M., Zhang, D., Shupe, M. D., Luke, E., and Protat, A.: Understanding Rapid Changes in Phase Partitioning between Cloud Liquid and Ice in Stratiform Mixed-Phase Clouds: An Arctic Case Study., Monthly Weather Review, 144, 4805 – 4826, http://search.ebscohost.com/login.aspx?direct=true&db=asn&AN=119879777&site=ehost-live, 2016.

Kay, J. E., L'Ecuyer, T., Chepfer, H., Loeb, N., Morrison, A., and Cesana, G.: Recent Advances in Arctic Cloud and Climate Research, Current Climate Change Reports, 2, 159–169, https://doi.org/10.1007/s40641-016-0051-9, 2016.

Kiszler, T., Ebell, K., and Schemann, V.: A Performance Baseline for the Representation of Clouds and Humidity in Cloud-Resolving ICON-LEM Simulations in the Arctic, Journal of Advances in Modeling Earth Systems, 15, e2022MS003 299, https://doi.org/https://doi.org/10.1029/2022MS003299, e2022MS003299 2022MS003299, 2023.

Komurcu, M., Storelvmo, T., Tan, I., Lohmann, U., Yun, Y., Penner, J. E., Wang, Y., Liu, X., and Takemura, T.: Intercomparison of the cloud water phase among global climate models, Journal of Geophysical Research: Atmospheres, 119, 3372–3400, https://doi.org/https://doi.org/10.1002/2013JD021119, 2014.

Korolev, A., McFarquhar, G., Field, P. R., Franklin, C., Lawson, P., Wang, Z., Williams, E., Abel, S. J., Axisa, D., Borrmann, S., Crosier, J., Fugal, J., Krämer, M., Lohmann, U., Schlenczek, O., Schnaiter, M., and Wendisch, M.: Mixed-Phase Clouds: Progress and Challenges, Meteorological Monographs, 58, 5.1 – 5.50, https://doi.org/https://doi.org/10.1175/AMSMONOGRAPHS-D-17-0001.1, 2017.

Korolev, A. V.: Rates of phase transformations in mixed-phase clouds, Q.J.R. Meteorol. Soc., 134, 595–608, https://doi.org/10.1002/qj.230, 2008.

Lasher-Trapp, S., Kumar, S., Moser, D. H., Blyth, A. M., French, J. R., Jackson, R. C., Leon, D. C., and Plummer, D. M.: On Different Microphysical Pathways to Convective Rainfall, Journal of Applied Meteorology and Climatology, 57, 2399 – 2417, https://doi.org/https://doi.org/10.1175/JAMC-D-18-0041.1, 2018.

McGraw, Z., Storelvmo, T., Polvani, L. M., Hofer, S., Shaw, J. K., and Gettelman, A.: On the Links Between Ice Nucleation, Cloud Phase, and Climate Sensitivity in CESM2, Geophysical Research Letters, 50, e2023GL105 053, https://doi.org/https://doi.org/10.1029/2023GL105053, e2023GL105053 2023GL105053, 2023.

Middlemas, E. A., Kay, J. E., Medeiros, B. M., and Maroon, E. A.: Quantifying the Influence of Cloud Radiative Feedbacks on Arctic Surface Warming Using Cloud Locking in an Earth System Model, Geophysical Research Letters, 47, e2020GL089 207, https://doi.org/10.1029/2020GL089207, e2020GL089207 2020GL089207, 2020.

Mioche, G., Jourdan, O., and Ceccaldi, M.: Variability of mixed-phase clouds in the Arctic with a focus on the Svalbard region: a study based on spaceborne active remote sensing, Atmospheric Chemistry and Physics, 15, 2445, 2015.

Mitchell, J. F. B., Senior, C. A., and Ingram, W. J.: C02 and climate: a missing feedback?, Nature, 341, 132–134, https://doi.org/10.1038/341132a0, 1989.

Morrison, H., van Lier-Walqui, M., Fridlind, A. M., Grabowski, W. W., Harrington, J. Y., Hoose, C., Korolev, A., Kumjian, M. R., Milbrandt, J. A., Pawlowska, H., Posselt, D. J., Prat, O. P., Reimel, K. J., Shima, S.-I., van Diedenhoven, B., and Xue, L.: Confronting the Challenge of Modeling Cloud and Precipitation Microphysics, Journal of Advances in Modeling Earth Systems, 12, e2019MS001 689, https://doi.org/https://doi.org/10.1029/2019MS001689, e2019MS001689 2019MS001689, 2020.

Nomokonova, T., Ebell, K., Löhnert, U., Maturilli, M., Ritter, C., and O'Connor, E.: Statistics on clouds and their relation to thermodynamic conditions at Ny-Ålesund using ground-based sensor synergy, Atmospheric Chemistry and Physics, 19, 4105–4126, https://doi.org/10.5194/acp-19-4105-2019, 2019.

Phillips, V. T. J., DeMott, P. J., and Andronache, C.: An Empirical Parameterization of Heterogeneous Ice Nucleation for Multiple Chemical Species of Aerosol, Journal of the Atmospheric Sciences, 65, 2757 – 2783, https://doi.org/https://doi.org/10.1175/2007JAS2546.1, 2008.

Rantanen, M., Karpechko, A. Y., Lipponen, A., Nordling, K., Hyvärinen, O., Ruosteenoja, K., Vihma, T., and Laaksonen, A.: The Arctic has warmed nearly four times faster than the globe since 1979, Communications Earth & Environment, 3, 168, https://doi.org/10.1038/s43247-022-00498-3, 2022.

Schemann, V. and Ebell, K.: Simulation of mixed-phase clouds with the ICON large-eddy model in the complex Arctic environment around Ny-Ålesund, Atmospheric Chemistry and Physics, 20, 475–485, https://doi.org/10.5194/acp-20-475-2020, 2020.

Segal, Y. and Khain, A.: Dependence of droplet concentration on aerosol conditions in different cloud types: Application to droplet concentration parameterization of aerosol conditions, Journal of Geophysical Research: Atmospheres, 111, https://doi.org/https://doi.org/10.1029/2005JD006561, 2006.

Seifert, A. and Beheng, K. D.: A two-moment cloud microphysics parameterization for mixed-phase clouds. Part 1: Model description, Meteorology and Atmospheric Physics, 92, 45–66, https://doi.org/10.1007/s00703-005-0112-4, 2006.

Shaw, J., McGraw, Z., Bruno, O., Storelvmo, T., and Hofer, S.: Using Satellite Observations to Evaluate Model Microphysical Representation of Arctic Mixed-Phase Clouds, Geophysical Research Letters, 49, e2021GL096 191, https://doi.org/https://doi.org/10.1029/2021GL096191, e2021GL096191 2021GL096191, 2022.

Shupe, M. D. and Intrieri, J. M.: Cloud Radiative Forcing of the Arctic Surface: The Influence of Cloud Properties, Surface Albedo, and Solar Zenith Angle, Journal of Climate, 17, 616 – 628, https://doi.org/https://doi.org/10.1175/1520-0442(2004)017<0616:CRFOTA>2.0.CO;2, 2004.

Shupe, M. D., Kollias, P., Persson, P. O. G., and McFarquhar, G. M.: Vertical Motions in Arctic Mixed-Phase Stratiform Clouds, Journal of the Atmospheric Sciences, 65, 1304–1322, https://doi.org/10.1175/2007JAS2479.1, 2008.

Storelvmo, T. and Tan, I.: The Wegener-Bergeron-Findeisen process ? Its discovery and vital importance for weather and climate, Meteorologische Zeitschrift, 24, 455–461, https://doi.org/10.1127/metz/2015/0626, 2015.

Storelvmo, T., Tan, I., and Korolev, A. V.: Cloud Phase Changes Induced by CO2 Warming—a Powerful yet Poorly Constrained Cloud-Climate Feedback, Current Climate Change Reports, 1, 288–296, https://api.semanticscholar.org/CorpusID:22718554, 2015.

Tan, I., Storelvmo, T., and Zelinka, M. D.: Observational constraints on mixed-phase clouds imply higher climate sensitivity, Science, 352, 224–227, https://doi.org/10.1126/science.aad5300, 2016.

Wang, Y., Liu, X., Hoose, C., and Wang, B.: Different contact angle distributions for heterogeneous ice nucleation in the Community Atmospheric Model version 5, Atmospheric Chemistry and Physics, 14, 10 411–10 430, https://doi.org/10.5194/acp-14-10411-2014, 2014.

Zelinka, M. D., Myers, T. A., McCoy, D. T., Po-Chedley, S., Caldwell, P. M., Ceppi, P., Klein, S. A., and Taylor, K. E.: Causes of Higher Climate Sensitivity in CMIP6 Models, Geophysical Research Letters, 47, e2019GL085 782, https://doi.org/https://doi.org/10.1029/2019GL085782, e2019GL085782 10.1029/2019GL085782, 2020.

Zhang, M., Xie, S., Liu, X., Lin, W., Zhang, K., Ma, H.-Y., Zheng, X., and Zhang, Y.: Toward Understanding the Simulated Phase Partitioning of Arctic Single-Layer Mixed-Phase Clouds in E3SM, Earth and Space Science, 7, e2020EA001 125, https://doi.org/https://doi.org/10.1029/2020EA001125, e2020EA001125 2020EA001125, 2020.